

Why Pass@k Optimization Can Degrade Pass@1: Prompt Interference in LLM Post-training

Anas Barakat¹, Souradip Chakraborty², Khushbu Pahwa^{*}, Amrit Singh Bedi³

¹Singapore University of Technology and Design ²University of Maryland, College Park

³University of Central Florida

Pass@k is a widely used performance metric for verifiable large language model tasks, including mathematical reasoning, code generation, and short-answer reasoning. It defines success if any of k independently sampled solutions passes a verifier. This multi-sample inference metric has motivated inference-aware fine-tuning methods that directly optimize pass@k. However, prior work reports a recurring trade-off: pass@k improves while pass@1 degrades under such methods. This trade-off is practically important because pass@1 often remains a hard operational constraint due to latency and cost budgets, imperfect verifier coverage, and the need for a reliable single-shot fallback. We study the origin of this trade-off and provide a theoretical characterization of when pass@k policy optimization can reduce pass@1 through gradient conflict induced by prompt interference. We show that pass@k policy gradients can conflict with pass@1 gradients because pass@k optimization implicitly reweights prompts toward low-success prompts; when these prompts are what we term *negatively interfering*, their upweighting can rotate the pass@k update direction away from the pass@1 direction. We illustrate our theoretical findings with large language model experiments on verifiable mathematical reasoning tasks.

1. Introduction

Pass@k optimization. In many verifiable tasks, such as code generation and short-answer math, a system can afford multiple response attempts for the same prompt and check the correctness of each response attempt with an automatic verifier (e.g., unit tests, exact-match) that can check the correctness of generated answers. This naturally leads to *pass@k inference*: sample k independent candidate solutions and declare success if *any* candidate is correct. The corresponding metric, pass@k, measures the probability that at least one of k i.i.d. samples solves the prompt, and has become a standard performance measure when multiple attempts are available (Chen et al., 2021; Gehring et al., 2025; Li et al., 2022). This “ k attempts with verification” setting suggests that the training objective should align with deployment: if inference uses k attempts, training should directly optimize the same pass@k objective rather than optimizing only the single-sample expected reward. Recent work develops policy-gradient estimators and practical training procedures that optimize pass@k, and demonstrates large gains in pass@k performance on reasoning and code benchmarks (Tang et al., 2025; Walder and Karkhanis, 2025).

Trade-off: optimizing pass@k can reduce pass@1. A key complication is that pass@k optimization does not necessarily improve single-shot pass@1 performance. Empirically, some recent works report objective-dependent trade-offs where pass@k improves while pass@1 drops (Tang et al., 2025; Walder and Karkhanis, 2025). For example, Walder and Karkhanis (2025) explicitly highlight a trade-off between pass@1 and pass@k during code-generation fine-tuning (e.g. Tables 1 to 4 in their paper), and their results show that optimizing a pass@k objective can lower pass@1 even as higher- k metrics increase substantially (Table 1). These regressions make pass@k optimization risky in settings where single-shot accuracy is a hard requirement.

*Work does not relate to position at Amazon.

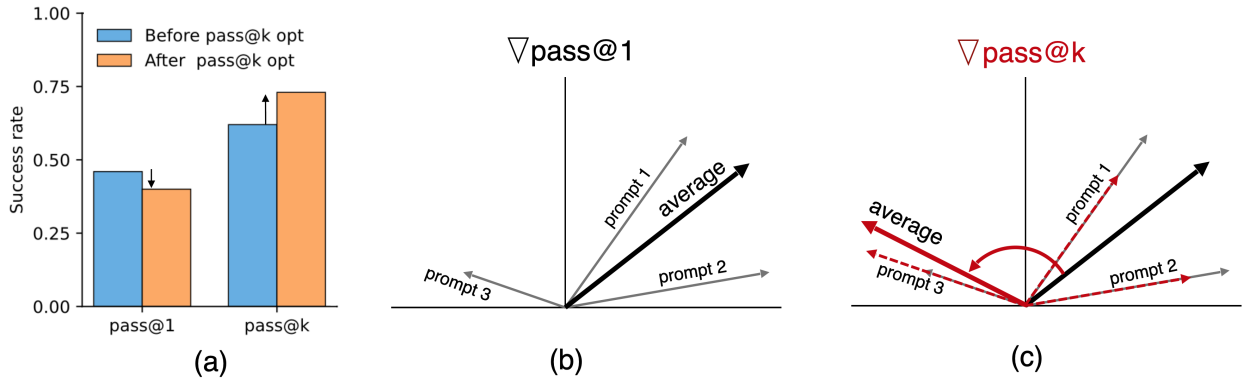


Figure 1 | **(a) Empirical trade-off.** Under pass@k policy optimization, pass@k increases while pass@1 may decrease. We explain this empirically observed trade-off in (b) and (c), which schematically illustrate the pass@1 and pass@k ($k > 1$) gradients for three prompts and their expectations in policy-parameter space. **(b) Pass@1 gradients with negatively interfering prompt.** This panel shows a setting in which prompt 3 is *negatively interfering* with prompts 1 and 2, i.e., the per-prompt pass@1 gradient for prompt 3 has negative inner product with the per-prompt pass@1 gradients for prompts 1 and 2 (see Section 3). Here, $\nabla \text{pass}@1$ denotes the population pass@1 gradient, given by the average (expectation over prompts; here under a uniform distribution) of the per-prompt pass@1 gradients. **(c) Pass@k vs pass@1 gradient conflict.** Per-prompt pass@k gradients are scaled versions of the corresponding per-prompt pass@1 gradients (Eq. (2)). This reweighting amplifies the magnitude of the pass@k gradient for the negatively interfering prompt 3, causing the resulting population pass@k gradient to conflict with the population pass@1 gradient (their inner product becomes negative, corresponding to an obtuse angle, shown here as approximately 120°). Consequently, a policy update in the pass@k gradient direction can increase pass@k while decreasing pass@1.

Why this degradation matters. Pass@1 remains operationally important: many deployments have limited latency or cost budgets, may not have reliable verifiers for every prompt, and often need a strong single-shot fallback even when retries are possible. In these regimes, a training procedure that improves pass@k at the cost of pass@1 can reduce overall system reliability and complicate model selection and deployment.

Open question. Despite growing adoption of pass@k objectives, it is still not well understood *why* pass@k optimization can hurt pass@1, and *when* we should expect this trade-off to appear. Without a principled explanation, it is difficult to design reliable inference-aware fine-tuning methods that deliver multi-attempt gains while preserving strong single-shot performance. This leads to our research question:

When and why can pass@k policy optimization degrade pass@1 performance?

Our key insight. Compared to pass@1, optimizing the pass@k objective induces an implicit *prompt reweighting* toward prompts with lower success probability (i.e., prompts the current policy rarely solves). When these prompts contribute gradients that conflict with the population pass@1 gradient, upweighting them increases their influence on the pass@k policy gradient update. Consequently, the pass@k gradient can conflict with the pass@1 gradient direction. In this regime, pass@k improves under pass@k updates while pass@1 decreases (see Figure 1 for a schematic explanation). We identify the prompts that can lead to gradient conflict as negatively interfering using the concept of *prompt interference* we introduce in this work.

Our main contributions are as follows:

- **Prompt interference.** We introduce the concept of prompt interference. We say that two given prompts are positively (resp. negatively) interfering if a policy parameter update which increases the probability of providing a correct response for that prompt tends to increase (resp. decrease) the probability of success of the other prompt. To capture the similarity between prompts in terms of pass@1 gradient representation, we introduce a similarity kernel to define the concept of prompt interference mathematically. The induced distribution over negatively interfering prompts is crucial to understand the pass@k and pass@1 trade-off.
- **Gradient conflict characterization.** We show that pass@k and pass@1 gradients can be conflicting in the sense that they can form an obtuse angle. This implies that a policy update following pass@k’s policy gradient tends to increase pass@k while decreasing pass@1. We provide a characterization of this gradient conflict by establishing an interpretable expression for the inner product between pass@k and pass@1. This characterization crucially uses the fact that per-prompt pass@k gradients are *weighted* pass@1 per-prompt policy gradients. The gradient conflict expression shows that gradient conflict occurs when negatively interfering prompt regions are upweighted by the implicit pass@k reweighting and hence dominate the contribution of positively interfering prompts.
- **Sufficient conditions and influence of k .** Using our gradient conflict characterization, we provide sufficient conditions under which gradient conflict occurs. We further study the influence of the parameter k and show that increasing k encourages gradient conflict under some conditions in the relative probability of success in negatively versus positively interfering prompts.
- **Pass@1 degradation under pass@k updates.** We prove that pass@1 decreases while pass@k increases (simultaneously) under one-step pass@k policy updates satisfying an explicit stepsize condition. To show this result, we establish and use smoothness of the pass@k objective under a standard policy parameter regularity assumption.
- **Empirical validation.** We illustrate our main findings on large language models for solving math reasoning questions.

2. Preliminaries

In this section, we formally define the pass@k objective and recall its policy gradients as used in pass@k policy optimization. We consider a setting where a language model is represented as a stochastic policy π_θ parameterized by weights $\theta \in \mathbb{R}^d$ over a set of responses \mathcal{Y} given a set of prompts denoted by \mathcal{X} (e.g., math questions). The conditional probability distribution of the model’s output responses when prompted with x is $\pi_\theta(\cdot|x)$. We denote by \mathcal{D} the distribution over prompts.

Pass@k objective. Given a prompt x sampled from a distribution \mathcal{D} , a single ‘attempt’ is a response $y \sim \pi_\theta(\cdot|x)$. We suppose we have access to a binary reward verifier $r(x, y) \in \{0, 1\}$ which encodes correctness of response y for prompt x . The per-prompt success probability for any $x \in \mathcal{X}$ and any policy parameter $\theta \in \mathbb{R}^d$ will be denoted:

$$p_\theta(x) := \mathbb{E}_{y \sim \pi_\theta(\cdot|x)}[r(x, y)] = \mathbb{P}_{y \sim \pi_\theta(\cdot|x)}(r(x, y) = 1), \quad (1)$$

where the last identity follows from the fact that rewards are binary ($r(x, y) \in \{0, 1\}$). The pass@k objective is defined as the probability that at least one response is correct among k responses, i.e.,

$$J_k(\theta) := \mathbb{P}\left(\max_{1 \leq i \leq k} r(x, y_i) = 1\right) = \mathbb{E}_{x \sim \mathcal{D}}[1 - (1 - p_\theta(x))^k], \quad (\text{pass@k})$$

where $x \sim \mathcal{D}$, $y_i \sim \pi_\theta(\cdot|x)$ for $i = 1, \dots, k$ are k independent response samples. Hence pass@k can be written using the nonlinear transformation $f_k(p) := 1 - (1 - p)^k$ as $J_k(\theta) = \mathbb{E}_{x \sim \mathcal{D}}[f_k(p_\theta(x))]$. It

immediately follows that pass@k is an increasing function in k : $\forall m \geq k \geq 1, \forall \theta \in \mathbb{R}^d, J_m(\theta) \geq J_k(\theta)$. Moreover, pass@k can be bounded by pass@1 using Jensen’s inequality and concavity of f_k w.r.t. its argument: for all $k \geq 1, \theta \in \mathbb{R}^d, J_1(\theta) \leq J_k(\theta) \leq \min(1, f_k(J_1(\theta)))$. Note that under our notation $J_1(\theta) = \mathbb{E}_{x \sim \mathcal{D}}[p_\theta(x)]$.

Pass@k policy gradients. Pass@k optimization can be performed using pass@k policy gradients. It follows from the chain rule that the gradient of pass@k w.r.t. the policy parameters is given by:

$$\nabla J_k(\theta) = \mathbb{E}_{x \sim \mathcal{D}}[w_k(p_\theta(x)) \nabla p_\theta(x)], w_k(p) := k(1 - p)^{k-1}, \quad (2)$$

as noted in a few recent works (Mahdavi et al., 2025; Yu, 2025). Pass@k gradients reweight prompts by

$$w_{k,\theta}(x) := w_k(p_\theta(x)) = k(1 - p_\theta(x))^{k-1}. \quad (3)$$

This weighting emphasizes low-probability of success prompts and downweights prompts with high probability of success. To compute pass@k gradients in (2), note that the gradient $\nabla p_\theta(x)$ of the prompt-wise probability of success for any prompt $x \in \mathcal{X}$ and any policy parameter $\theta \in \mathbb{R}^d$ immediately follows from (1) and is given by:

$$\nabla p_\theta(x) = \mathbb{E}_{y \sim \pi_\theta(\cdot|x)}[r(x, y) s_\theta(x, y)], \quad (4)$$

where $s_\theta(x, y) := \nabla \log \pi_\theta(y|x)$ denotes the score function.

This gradient expression has been recently used in Tang et al. (2025); Walder and Karkhanis (2025) for instance. Per-prompt pass@k and pass@1 are positively collinear as $\nabla J_k(x; \theta) := w_{k,\theta}(x) \nabla p_\theta(x) = w_{k,\theta}(x) \nabla J_1(x; \theta)$ and $w_{k,\theta}(x)$. However we will crucially see that pass@k and pass@1 as *expectation over prompts* will not necessarily be positively collinear. This discrepancy which was overlooked in the literature highlights the importance of the expectation over prompts and the structure of per-prompt pass@1 gradients. This motivates our next main section in which we introduce the concept of *prompt interference* capturing the potential conflict between the diversity of prompts in the underlying prompt distribution and the shared policy parameters across prompts.

3. Prompt Interference

In this section, we introduce the phenomenon of *prompt interference* which will play an important role in explaining later in the paper why pass@1 can degrade under pass@k policy updates. This section is focused on understanding the structure of pass@1 policy gradients over the set of prompts. The role of the pass@k objective and its influence on optimization will be discussed in section 4.

3.1. Prompt similarity measure and interference

The pass@1 objective is defined as the expectation of the per-prompt probability of success with respect to the distribution of prompts (see pass@k with $k = 1$). As a function of policy parameters, this pass@1 objective induces a shared-parameter coupling across prompts: the same policy parameters are shared across the entire distribution of prompts which might be diverse. As a consequence, a (shared) policy parameter update can improve the probability of success ($p_\theta(x)$) on some prompts while it can degrade it on other prompts. When this negative transfer occurs, we say that there is negative prompt interference. We provide a formal definition of this phenomenon in the rest of this section.

To define prompt interference, we investigate the structure of the pass@1 policy gradient, looking at the *per-prompt* pass@1 policy gradients and comparing them across prompts. We define the following

natural prompt gradient similarity measure $\kappa_\theta : \mathcal{X} \times \mathcal{X} \rightarrow \mathbb{R}$ defined for any policy parameter $\theta \in \mathbb{R}^d$ and any prompts $x, x' \in \mathcal{X}$ by:

$$\kappa_\theta(x, x') := \langle \nabla p_\theta(x), \nabla p_\theta(x') \rangle. \quad (5)$$

This kernel captures similarities between prompts in terms of their pass@1 gradients which encode their ability to improve the probability of success. Using the policy gradient expressions of the gradients of pass@1 in (4), we obtain:

$$\kappa_\theta(x, x') = \mathbb{E}_{y \sim \pi_\theta(\cdot|x), y' \sim \pi_\theta(\cdot|x')} [\delta(x, y, x', y') \langle s_\theta(x, y), s_\theta(x', y') \rangle], \quad (6)$$

where $\delta(x, y, x', y') := r(x, y) r(x', y')$ which is equal to 1 if and only if both y, y' are correct completions for x, x' respectively (as rewards are binary). The kernel informs on whether improving pass@1 on one prompt tends to also improve pass@1 on another prompt under the shared policy parameters. To see this, consider a policy update $\theta' = \theta + \eta \nabla p_\theta(x)$ with a small stepsize $\eta > 0$ in the direction $\nabla p_\theta(x)$ improving the probability of success on x . A first-order Taylor expansion of $\theta \mapsto p_\theta(x')$ gives:

$$p_{\theta'}(x') \simeq p_\theta(x') + \eta \langle \nabla p_\theta(x'), \nabla p_\theta(x) \rangle = p_\theta(x') + \eta \kappa_\theta(x', x).$$

This leads us to the following prompt interference definition.

Definition 3.1 (Prompt interference). We will say that two prompts x and x' are *interfering positively* if $\kappa_\theta(x', x) > 0$: a step that increases the per-prompt pass@1 $p_\theta(x)$ at x also tends to increase $p_\theta(x')$. Otherwise, if $\kappa_\theta(x', x) < 0$, the two prompts will be said to *interfer negatively* and a step that increases $p_\theta(x)$ tends to decrease $p_\theta(x')$.

In the next section, we illustrate the prompt interference concept on a toy example.

3.2. Toy example

Setting. We consider a minimal contextual-bandit abstraction of verifier-based multi-sample LLM evaluation as a running example. A prompt is a context $x \in \mathcal{X}$ drawn from a mixture distribution with a latent difficulty label $\ell(x) \in \{\text{easy}, \text{hard}\}$ with a fixed proportion of hard labels: $\mathbb{P}(\ell(x) = \text{hard}) = p_{\text{hard}}$. Each prompt is represented by a 2D feature vector $\psi(x) = [1, s(x)]^\top \in \mathbb{R}^2$ with a bias 1 and a scalar feature $s(x) \in \mathbb{R}$. Conditioned on difficulty, the scalar feature follows overlapping Gaussians whose separation is controlled by a parameter $\delta > 0$: if $\ell(x) = \text{easy}$ then $s(x) \sim \mathcal{N}(-\delta/2, 1)$, and if $\ell(x) = \text{hard}$ then $s(x) \sim \mathcal{N}(+\delta/2, 1)$. Smaller δ yields greater overlap between easy and hard feature distributions. A completion is represented as a discrete action $y \in \{0, 1\}$. Each prompt has a unique correct completion determined by its difficulty: $y^*(x) = 0$ if $\ell(x) = \text{easy}$ and $y^*(x) = 1$ if $\ell(x) = \text{hard}$. The verifier reward is deterministic binary: $r(x, y) = \mathbf{1}\{y = y^*(x)\}$. We use a two-action softmax policy parameterized by a single vector $\theta \in \mathbb{R}^2$ such that $\pi_\theta(1|x) = \sigma(\theta^\top \psi(x))$ and $\pi_\theta(0|x) = 1 - \sigma(\theta^\top \psi(x))$, where $\sigma(t) = \frac{1}{1 + \exp(-t)}$ is the sigmoid function. The policy shares parameters across heterogeneous subpopulations (easy vs hard). For later use, we also note that we initialize the policy at a reference policy θ_{ref} that is globally biased toward action $y = 0$, inducing high initial success on easy prompts and low initial success on hard prompts.

Illustration of negative prompt interference. It follows that the per-prompt success probability defined in (1) is given by $p_\theta(x) = \pi_\theta(y^*(x)|x)$ for any prompt $x \in \mathcal{X}$. A simple computation yields:

$$\nabla p_\theta(x) = \begin{cases} -z_\theta(x) \psi(x), & \text{if } \ell(x) = \text{easy}, \\ +z_\theta(x) \psi(x), & \text{if } \ell(x) = \text{hard}, \end{cases} \quad (7)$$

where $z_\theta(x) := \sigma(\theta^\top \psi(x))(1 - \sigma(\theta^\top \psi(x))) \geq 0$. As a consequence, two prompts that have a similar representation will have opposite per-prompt pass@1 gradients and will hence be negatively interfering. This will be the case in our example for prompts in the overlap between the two Gaussians: two such prompts can have different labels (hard and easy) while having a similar prompt representation (with a similar scalar feature $s(x)$). See Figure 2 below for an illustration.

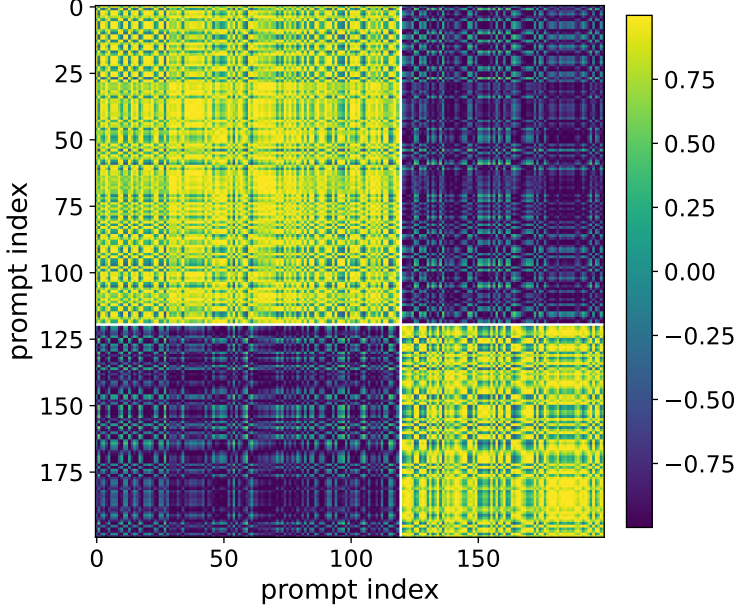


Figure 2 | Cosine kernel heatmap: $\cos(\nabla p_\theta(x), \nabla p_\theta(x'))$ for subsamples of prompts: 120 easy and 80 hard among a total of 6000 samples. Blue regions correspond to negative prompt interference.

In the next section, we show in our toy example how negative prompt interference can lead to pass@1 decrease under one-step pass@k policy gradient ascent.

3.3. Tradeoff: pass@k ascent can decrease pass@1

Using the toy example introduced in the previous section, we show in this section that pass@1 can decrease under one-step pass@k policy gradient ascent.

Fix $\delta = 0.2$ and consider two realized prompts in the overlap region between the 2 Gaussians: a prompt x_e with $\ell(x_e) = \text{easy}$ and $\psi(x_e) = [1, -0.1]^\top$, and x_h with $\ell(x_h) = \text{hard}$ and $\psi(x_h) = [1, +0.1]^\top$. These two prompts have nearly identical representations as $\cos(\psi(x_e), \psi(x_h)) \simeq 0.98$ is close to 1. Because of (7), they are therefore negative interfering as $\kappa_\theta(x_e, x_h) = \langle \nabla p_\theta(x_e), \nabla p_\theta(x_h) \rangle = -z_\theta(x_e)z_\theta(x_h)\langle \psi(x_e), \psi(x_h) \rangle < 0$ since $\langle \psi(x_e), \psi(x_h) \rangle > 0$. Numerically we have $\kappa_\theta(x_e, x_h) \simeq -0.01$ and $\cos(\nabla p_\theta(x_e), \nabla p_\theta(x_h)) \simeq -0.98$ which means that the per-prompt pass@1 gradients are almost antiparallel. On this two-point empirical distribution, the pass@1 and pass@k gradients are given by:

$$\begin{aligned} \nabla J_1(\theta) &= \frac{1}{2}(\nabla p_\theta(x_e) + \nabla p_\theta(x_h)), \\ \nabla J_{10}(\theta) &= \frac{1}{2}(w_e \nabla p_\theta(x_e) + w_h \nabla p_\theta(x_h)), \end{aligned}$$

where the pass@10 weight $w_e := w_{10,\theta}(x_e) \simeq 2.33 \times 10^{-7}$ whereas $w_h := w_{10,\theta}(x_h) \simeq 3.88$. Pass@10 upweights the hard prompt ($p_\theta(x_h) \simeq 0.10$ low) and aggressively downweights the easy prompt x_e (large $p_\theta(x_e) \simeq 0.86$). Indeed, recall that $w_{k,\theta}(x) = k(1 - p_\theta(x))^{k-1}$ which is near k when $p_\theta(x) \simeq 0$

but and near 0 when $p_\theta(x) \approx 1$. As a consequence, the pass@10 gradient is therefore dominated by $\nabla p_\theta(x_h)$ which conflicts with $\nabla p_\theta(x_e)$. Importantly, we have $\cos(\nabla J_1(\theta), \nabla J_{10}(\theta)) = -0.77 < 0$ meaning that the pass@1 and pass@10 are conflicting and strongly anti-aligned. With one gradient-ascent step on pass@10 $\theta^+ = \theta + \eta \nabla J_{10}(\theta)$ with $\eta = 5$, we have:

$$\begin{aligned} J_1(\theta) \simeq 0.48 &\rightarrow J_1(\theta^+) \simeq 0.46 \quad (\downarrow), \\ J_{10}(\theta) \simeq 0.83 &\rightarrow J_{10}(\theta^+) = 0.95 \quad (\uparrow). \end{aligned}$$

This shows that pass@1 decreases while pass@k increases under pass@k optimization. In our toy example, we have observed that negative prompt interference can induce a conflict between pass@1 and pass@k gradients when it is amplified by the induced pass@k prompt reweighting. In the next section, we go beyond our toy example to characterize this conflict between pass@k and pass@1 gradients in the general setting.

4. Pass@k and Pass@1 Gradients Conflict

In this section, we exploit the observation that pass@k policy optimization induces an implicit prompt reweighting, biased toward upweighting low-success prompts. To connect with the previous section, if this reweighting coincides with upweighting negatively interfering prompts, then pass@k policy updates may result in conflicting pass@k and pass@1 gradients, leading to pass@1 degradation under pass@k policy optimization updates. We make this chain of arguments precise in this section.

4.1. Gradient conflict: Reweighting meets interference

To explain why optimizing pass@k can hurt pass@1, we study a key quantity: the angle between the policy gradients of pass@k and pass@1 respectively. We show that this angle can be obtuse and we refer to this setting as a case of *conflicting gradients*.

This observation might seem a little surprising from the theory viewpoint at first glance. Indeed, the per-prompt gradient $\nabla J_k(x; \theta)$ of pass@k is always a positive multiple of the per-prompt policy gradient $\nabla J_1(x; \theta)$ of pass@1 since $\nabla J_k(x; \theta) = w_{k,\theta}(x) \nabla J_1(x; \theta)$ and $w_{k,\theta}(x) \geq 0$ for any prompt $x \in \mathcal{X}$. Nevertheless, the population gradients $\nabla J_k(\theta) = \mathbb{E}[\nabla J_k(x; \theta)]$ and $\nabla J_1(\theta) = \mathbb{E}[\nabla J_1(x; \theta)]$ need not form an acute angle as their inner product can be negative as we will see.

The following proposition provides an explicit expression of this inner product to characterize the gradients conflict. To state this result, we introduce the prompt-wise gradient agreement score for pass@1 defined for any policy parameter $\theta \in \mathbb{R}^d$ and any prompt $x \in \mathcal{X}$ as follows:

$$a_\theta(x) := \langle \nabla J_1(x; \theta), \nabla J_1(\theta) \rangle = \mathbb{E}_{x' \sim \mathcal{D}}[\kappa_\theta(x, x')]. \quad (8)$$

This agreement score quantifies the prompt-level gradient interference with the average pass@1 objective. If $a_\theta(x) > 0$, that prompt's pass@1 gradient points in a direction that also improves average pass@1. If $a_\theta(x) < 0$, it is anti-aligned and improving that prompt's pass@1 tends to decrease population pass@1 under the shared policy parameters θ . Using this agreement score, our characterization is as follows.

Proposition 4.1 (Gradients conflict characterization). *For any $k \geq 1$ and any $\theta \in \mathbb{R}^d$,*

$$\langle \nabla J_k(\theta), \nabla J_1(\theta) \rangle = \mathbb{E}_{x \sim \mathcal{D}}[w_{k,\theta}(x) a_\theta(x)] \quad (9)$$

$$= \mathbb{E}[w_{k,\theta}(x)] \cdot \|\nabla J_1(\theta)\|^2 + \text{cov}(w_{k,\theta}(x), a_\theta(x)). \quad (10)$$

In particular, $\langle \nabla J_k(\theta), \nabla J_1(\theta) \rangle < 0$ is equivalent to each one of the following conditions:

- (i) $\mathbb{E}_{x \sim \mathcal{D}} [w_{k,\theta}(x) a_\theta(x)] < 0$,
- (ii) $\text{cov}(w_{k,\theta}(x), a_\theta(x)) < -\mathbb{E}[w_{k,\theta}(x)] \cdot \|\nabla J_1(\theta)\|^2$.

Discussion of conditions. We discuss each condition and provide two interpretations explaining gradients conflict and we refer the reader to figures 3 and 4 for illustrations on the toy example of section 3.2:

(i) *Prompt distribution shift: pass@k reweights prompts.* Recalling that the weights $w_{k,\theta}(x)$ are nonnegative, define the reweighted prompt distribution:

$$\tilde{\mathcal{D}}_{k,\theta}(dx) \propto w_{k,\theta}(x) \mathcal{D}(dx),$$

inducing the expectation $\mathbb{E}_{\tilde{\mathcal{D}}_{k,\theta}} [f(x)] = \frac{\mathbb{E}_{\mathcal{D}} [w_{k,\theta}(x) f(x)]}{\mathbb{E}_{\mathcal{D}} [w_{k,\theta}(x)]}$ for any measurable function f of the prompt random variable x .^{*} Note that the distribution $\tilde{\mathcal{D}}_{k,\theta}$ places higher mass on prompts with smaller success probability $p_\theta(x)$ (hard prompts) since $w_{k,\theta}(x)$ is decreasing in $p_\theta(x)$. Therefore, we can rewrite (9) as follows:

$$\langle \nabla J_k(\theta), \nabla J_1(\theta) \rangle = \mathbb{E}_{\mathcal{D}} [w_{k,\theta}(x)] \cdot \mathbb{E}_{\tilde{\mathcal{D}}_{k,\theta}} [a_\theta(x)], \quad (11)$$

and since $\mathbb{E}_{\mathcal{D}} [w_{k,\theta}(x)] > 0$ (as $w_{k,\theta}(x) \geq 0$ and not equal to zero a.e.), we obtain the following equivalence between $\langle \nabla J_k(\theta), \nabla J_1(\theta) \rangle < 0$ and $\mathbb{E}_{\tilde{\mathcal{D}}_{k,\theta}} [a_\theta(x)] < 0$.

This characterization shows that conflict of gradients of pass@1 and pass@k occurs if and only if the average of the agreement score $a_\theta(x)$ under the pass@k induced prompt distribution $\tilde{\mathcal{D}}_{k,\theta}$ is negative. In contrast note that $\mathbb{E}_{\mathcal{D}} [a_\theta(x)] = \|\nabla J_1(\theta)\|^2 \geq 0$. Pass@k changes the prompt weighting from \mathcal{D} to $\tilde{\mathcal{D}}_{k,\theta}$ and the average agreement under this shifted distribution can become negative.

In summary, we obtain the following causal chain: pass@k induces a prompt reweighting toward harder prompts (i.e. lower $p_\theta(x)$ since $w_{k,\theta}(x)$ decreases in $p_\theta(x)$). If hard prompts have negative agreement score $a_\theta(x)$ (i.e. per-prompt pass@1 gradients are conflicting with the pass@1 gradient) then the reweighted average agreement becomes negative and the gradient of pass@k and pass@1 form an obtuse angle as a consequence, i.e. they are conflicting.

(ii) *Covariance between weights and agreement scores.* The covariance $\text{cov}(w_{k,\theta}(x), a_\theta(x))$ captures the coupling between ‘how much pass@k emphasizes a prompt’ (via weight $w_{k,\theta}(x)$) and ‘whether that prompt helps pass@1’ (via alignment score $a_\theta(x)$). The covariance term quantifies whether pass@k’s hardness reweighting concentrates gradient mass on prompts whose success-probability gradients are anti-aligned with the pass@1 gradient. Conflict happens when this anti-aligned hard-prompt mass overwhelms the positive term. See Appendix A for more details.

Remark 4.2. For a more general discussion of the conflict between pass@k and pass@m gradients for any $k, m \geq 1$ using our kernel viewpoint, see Appendix B.

4.2. Sufficient conditions and threshold in k

We now provide sufficient conditions for pass@k and pass@1 gradients conflict, as a corollary of Proposition 4.1. Before stating this result, we make a standard smoothness assumption on the policy parameterization.

Assumption 4.3 (Lipschitz and smooth policy). There exist positive constants G, F s.t. for all prompts $x \in \mathcal{X}$, we have the expected score bounds:

$$\mathbb{E}_{y \sim \pi_\theta(\cdot|x)} [\|\nabla \log \pi_\theta(y|x)\|^2] \leq G^2, \quad \mathbb{E}_{y \sim \pi_\theta(\cdot|x)} [\|\nabla^2 \log \pi_\theta(y|x)\|] \leq F. \quad (12)$$

^{*}Note that the denominator is nonzero as the weights are not equal to zero a.e.

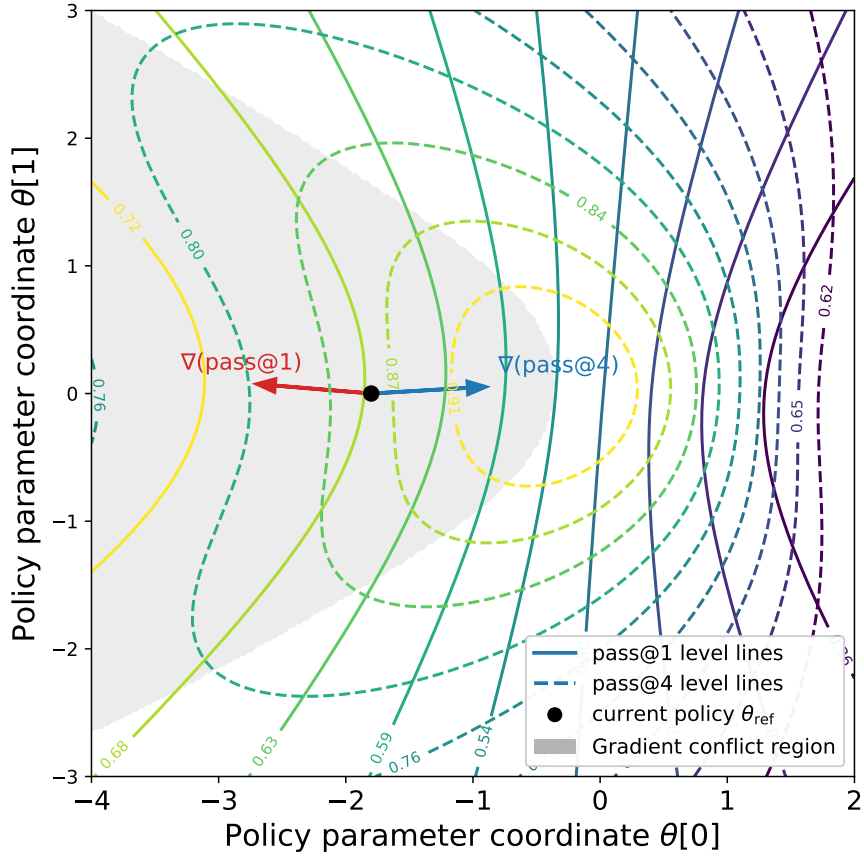


Figure 3 | Contour plots of pass@1 and pass@k objectives in the policy parameter space. Gradients of pass@k and pass@1 with respect to policy parameters are conflicting in the gray area.

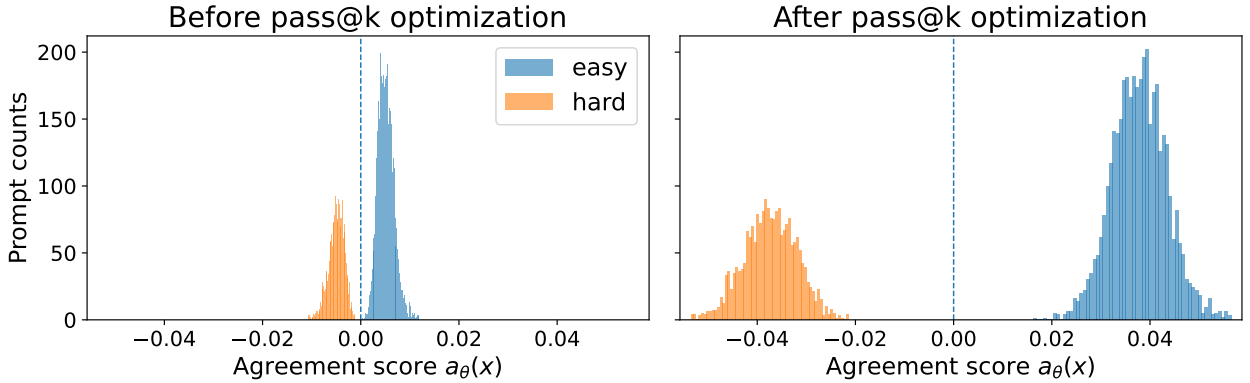


Figure 4 | Agreement score $a_{\theta}(x)$ (see (8)) on the toy example. The figure shows that the prompt distribution has both prompts with negative and positive agreement scores. Prompt with negative agreement scores are responsible for gradient conflict and hence pass@1 decrease. After pass@k policy optimization, negative agreement scores get even more negative.

This assumption is satisfied for instance by Gaussian policies with bounded state feature vectors and softmax tabular policies, see e.g. Lemma 4.4, 4.8 and corollary 4.3 in Yuan et al. (2022). This is a standard assumption in several works on the convergence analysis of policy gradient methods, see, e.g., Papini et al. (2022); Yuan et al. (2022).

To quantify the magnitude of negative interference and its prevalence under the distribution \mathcal{D} , we define the m -strongly negatively interfering prompt set with margin $m > 0$:

$$\mathcal{X}_-(\theta, m) := \{x \in \mathcal{X} : a_\theta(x) \leq -m\}, \quad (13)$$

and denote by $q_\theta := \mathcal{D}(\mathcal{X}_-(\theta, m)) \in [0, 1]$ its probability mass under the distribution \mathcal{D} of prompts. Then, the expected pass@k weight contributions inside and outside the m -strongly interfering set $\mathcal{X}_-(\theta, m)$ are given by:

$$W_-(k, \theta) := \mathbb{E}[w_{k,\theta}(x) \mathbb{1}_{\{x \in \mathcal{X}_-(\theta, m)\}}], \quad (14)$$

$$W_+(k, \theta) := \mathbb{E}[w_{k,\theta}(x) \mathbb{1}_{\{x \notin \mathcal{X}_-(\theta, m)\}}]. \quad (15)$$

The following corollary of Proposition 4.1 shows that gradients of pass@1 and pass@k conflict when the contribution of pass@k weights in negatively interfering prompt regions dominates its counterpart for positively interfering prompts.

Corollary 4.4 (Dominating negatively interfering prompts). *Let Assumption 4.3 hold. Suppose that $q_\theta > 0$ and let $k \geq 2$. Then for any $\theta \in \mathbb{R}^d$, $\langle \nabla J_k(\theta), \nabla J_1(\theta) \rangle \leq -\delta(\theta)$ where $\delta(\theta) := mW_-(k, \theta) - G^2W_+(k, \theta)$. If in addition $\delta(\theta) < 0$, then $\langle \nabla J_k(\theta), \nabla J_1(\theta) \rangle \leq -\delta(\theta) < 0$.*

Discussion of assumption. Note that the assumption $q_\theta > 0$ is necessary for gradient conflict. Indeed, if instead we have for instance for almost every $x \in \mathcal{X}$, $a_\theta(x) \geq 0$, then it follows from (9) that $\langle \nabla J_k(\theta), \nabla J_1(\theta) \rangle \geq 0$ as the weights $w_{k,\theta}(x)$ are also always nonnegative. Negative agreement score is a necessary condition for gradient conflict.

The gradient conflict condition of Corollary 4.4 depends on the relative weights contribution ratio $W_-(k, \theta)/W_+(k, \theta)$ in negative vs positive prompt agreement score regions. This ratio is a function of both the chosen parameter k and the probability of success $p_\theta(x)$ (1) under policy π_θ . We now exploit the closed form of the pass@k weights $w_{k,\theta}(x) := k(1 - p_\theta(x))^{k-1}$ to evaluate the ratio under assumptions on the prompt-wise probabilities of success. The next result shows that beyond a threshold k^* , the pass@k and pass@1 gradients form an obtuse angle. We make a separation assumption on the probability of success over prompts: the probability of success for m -strongly interfering prompts is supposed to be uniformly smaller than the probability of success of the remaining prompts. Intuitively, this boils down to assume that negatively interfering prompts are relatively harder to solve than the rest of the prompts.

Proposition 4.5 (Influence of k). *In the setting of corollary 4.4, assume there exist $\varepsilon, \delta, q > 0$ s.t.*

$$\sup_{x \in \mathcal{X}_-(m, \theta)} p_\theta(x) \leq \varepsilon < \delta \leq \inf_{x \notin \mathcal{X}_-(m, \theta)} p_\theta(x), \quad (16)$$

and $q_\theta \geq q$ for any θ , then $\langle \nabla J_k(\theta), \nabla J_1(\theta) \rangle \leq -\delta$ where $\delta = k[(1 - \varepsilon)^{k-1}mq - (1 - \delta)^{k-1}G^2(1 - q)]$. If in addition $k > k^* := 1 + \frac{\log(\frac{(1-q)G^2}{qm})}{\log(\frac{1-\varepsilon}{1-\delta})}$, then $\langle \nabla J_k(\theta), \nabla J_1(\theta) \rangle < 0$.

This result shows there is a phase transition in k : if k is large enough then gradients of pass@k and pass@1 will be conflicting and hence pass@1 will degrade while pass@k will improve under a small step size policy update following pass@k's gradient. The threshold k^* becomes smaller when the probability mass of the negatively interfering region is larger. This means that under larger negative prompt interference, the conflict between pass@1 and pass@k becomes more severe as it occurs for even smaller k .

4.3. Pass@1 degradation under pass@k updates

In this section, we show and quantify pass@1 decrease and pass@k increase under pass@k policy optimization, exploiting the conflict between pass@k and pass@1 gradients shown in the previous sections. To quantify improvement and degradation under policy updates, we prove smoothness of the pass@k objective for any $k \geq 1$ under Assumption 4.3 (see Lemma C.1 in appendix C.4). Using this smoothness property, we show that gradient conflict results in provable pass@1 decrease under pass@k optimization.

Proposition 4.6 (Pass@1 decrease under pass@k updates). *In the setting of corollary 4.4, set $\theta^+ = \theta + \eta \nabla J_k(\theta)$ where $k \geq 2$ and $\eta > 0$. If $\eta \leq \min(\frac{\delta(\theta)}{C_2}, \frac{1}{L_k})$ where $C_2 := k^2 G^2 L_1 / 2$ then*

$$J_1(\theta^+) < J_1(\theta) - \eta \delta(\theta) + C_2 \eta^2 < J_1(\theta), \quad (17)$$

$$J_k(\theta^+) \geq J_k(\theta) + \frac{\eta}{2} \|\nabla J_k(\theta)\|^2 \geq J_k(\theta). \quad (18)$$

The stepsize condition guarantees that the stepsize is small enough to ensure both decrease of pass@1 and increase of pass@k using the different smoothness constants of pass@k and pass@1 compared to the gradient conflict strength $\delta(\theta)$. See Figure 5 for an illustration over multiple iterations.

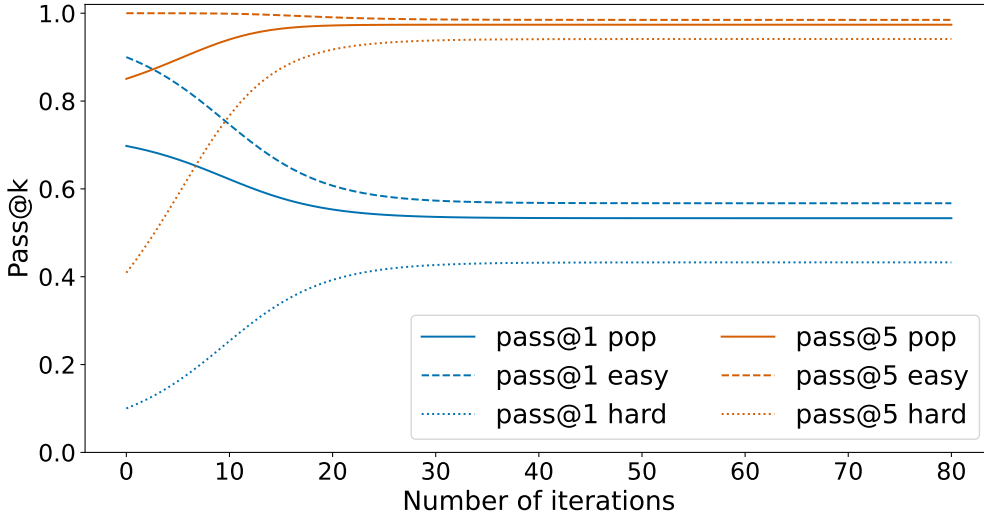


Figure 5 | Pass@5 vs pass@1 in example of section 3.2 with pass@5 policy optimization, ‘pop’ refers to ‘population’ i.e. pass@k as defined in (pass@k), ‘easy’ and ‘hard’ mean expectation is only taken over prompts labeled as easy respectively hard. Pass@5 increases while pass@1 decreases.

5. Experiments

We empirically test whether the pass@k objective can induce gradient conflict with pass@1 on math reasoning, as predicted by Proposition 4.1.

Dataset and models. We use the MATH dataset (Hendrycks et al., 2021), which contains competition-style high school math problems spanning seven subjects (Algebra, Counting & Probability, Geometry, Intermediate Algebra, Number Theory, Precalculus, and Prealgebra). We randomly sample 2,000 problems for evaluation. We run experiments with two reasoning models: DeepSeek-R1-Distill-Llama-8B and DeepSeek-R1-Distill-Qwen-7B.

Pass@k gradient computation. For computational efficiency, we compute pass@1 gradients with respect to policy parameters in the language model’s final hidden layer (dimension $d = 4096$ for Llama-8B, $d = 3584$ for Qwen-7B). We compute pass@k gradients using Monte Carlo estimates based on (2) and pass@k estimates developed in prior work (Chen et al., 2021; Walder and Karkhanis, 2025).

Setup. We create filtered data sets $\mathcal{D}_{\delta_1, \delta_2}$ of prompts and responses with varying difficulty thresholds (δ_1, δ_2) consisting of (i) hard prompts ($p_\theta(x_i) < \delta_2$) and (ii) easy prompts ($p_\theta(x_i) > \delta_1$). We test 7 combinations with $\delta_1 \in \{0.80, 0.85, 0.90\}$ and $\delta_2 \in \{0.05, 0.10, 0.15\}$. For each combination, we compute estimates of the agreement scores $a_\theta(x)$ as defined in (8), pass@k weights $w_{k, \theta}(x)$ (see (3)) and estimated average weighted agreement scores over prompts, which correspond to pass@k and pass@1 gradient inner product as shown in Proposition 4.1. See Appendix D.2 for all threshold configurations.

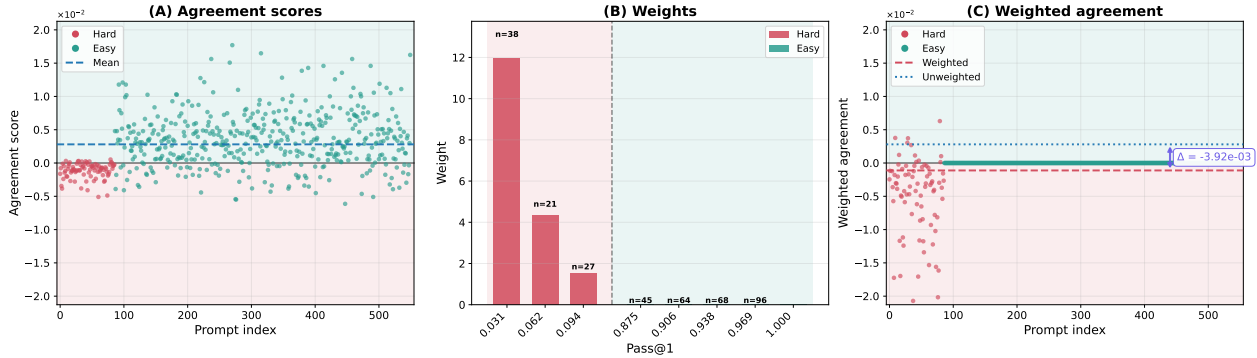
Discussion. Our experiments validate the theoretical predictions in several ways. First, the agreement scores (column A in Figure 6) show clear separation between hard prompts (red points, negative agreement scores clustered below zero) and easy prompts (green points, positive agreement scores above zero), confirming that prompt interference exists in practice. The unweighted mean agreement (blue dashed line) is positive, indicating that under uniform weighting, the population gradient would improve pass@1.

Second, the pass@k weights (column B in Figure 6) reveal extreme disparity in how pass@k values different prompts. The histogram shows that hard prompts (red bars, low pass@1 values $\lesssim 0.1$) receive weights of $n = 38$ at scale 12, $n = 21$ at scale 4, and $n = 27$ at scale 1, while easy prompts (green bars, high pass@1 values $\gtrsim 0.85$) receive negligible weights near 10^{-28} . This creates weight ratios exceeding $10^{28} : 1$, demonstrating the extreme reweighting mechanism our theory identifies: pass@k dramatically amplifies the influence of low-success prompts while effectively ignoring high-success prompts.

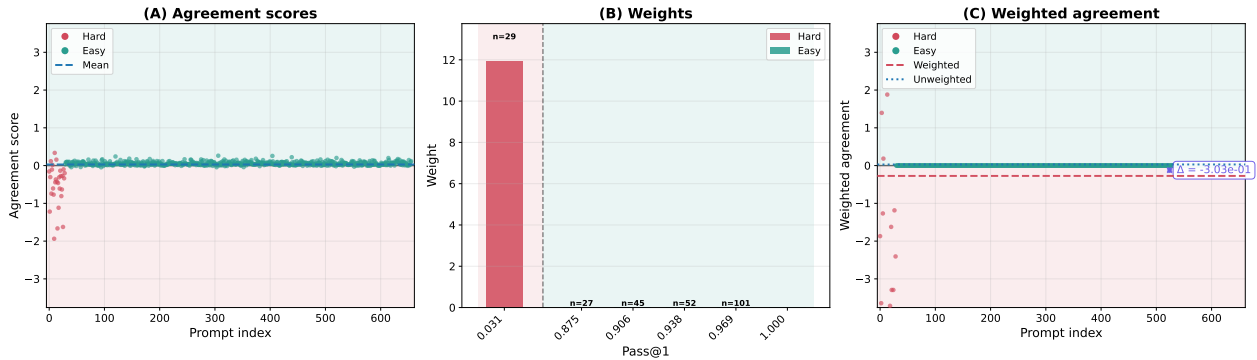
Third, column C demonstrates the consequence of this reweighting through weighted agreement scores. The purple arrows in panel C highlight the critical downward shift from the unweighted mean (blue dotted line, matching column A) to the weighted mean (red dashed line). For Llama-8B (Figure 6a, this shift is $\Delta = -3.92 \times 10^{-3}$, moving from $+2.80 \times 10^{-3}$ to -1.12×10^{-3} and flipping the gradient alignment from positive to negative, resulting in an inner product of -0.613). For Qwen-7B (Figure 6b), despite having only 29 hard prompts versus 627 easy prompts (a 21.6:1 ratio heavily favoring easy prompts), the extreme weight disparity causes an even more dramatic shift of $\Delta = -3.04 \times 10^{-1}$, moving from $+2.97 \times 10^{-2}$ to -2.74×10^{-1} , yielding a strongly negative inner product of -181 .

This validates Proposition 4.1: when the negative covariance between pass@k weights $w_{k, \theta}(x)$ and agreement scores $a_\theta(x)$ dominates the positive term $\mathbb{E}[w_{k, \theta}(x)] \cdot \|\nabla J_1(\theta)\|^2$, gradient conflict occurs. The visualization confirms our causal chain: pass@k upweights hard prompts (column B) \rightarrow these hard prompts exhibit negative interference $a_\theta(x) < 0$ (column A) \rightarrow the reweighted gradient conflicts with pass@1’s gradient (column C). The robustness across all seven threshold configurations (see Appendix D.2, Figure 8) demonstrates this is not an artifact of threshold selection but a fundamental property of pass@k optimization in the presence of negatively interfering prompts.

Additional ablations: Which prompts are amplified by pass@k? To have a complementary view of the amplification mechanism, we directly plot weights against agreement scores, with color encoding pass@1 probability. See Figure 7 which shows results for both models across three representative threshold configurations. The critical observation is where these weights concentrate in agreement-score space (x-axis). High-weight prompts cluster in the negative-agreement region ($a_\theta(x) < 0$), while



(a) DeepSeek-R1-Distill-Llama-8B: $\delta_1 = 0.85$, $\delta_2 = 0.10$ (550 prompts: 86 hard, 464 easy, ratio 5.4:1)



(b) DeepSeek-R1-Distill-Qwen-7B: $\delta_1 = 0.85$, $\delta_2 = 0.05$ (656 prompts: 29 hard, 627 easy, ratio 21.6:1)

Figure 6 | **Pass@k optimization hurts pass@1 performance: Gradient conflict across two models.** Both models demonstrate how pass@k reweighting causes gradient conflict with pass@1, despite different threshold settings. Agreement scores are computed relative to the pass@1 gradient of filtered prompts. **Left column (A):** Agreement scores show separation between hard negatives (red) and easy positives (green), with unweighted means shown as blue dashed lines. **Middle column (B):** Pass@k weights grouped by pass@1 probability, showing extreme weight disparity ($\sim 10^{28}:1$) between hard and easy prompts. **Right column (C):** Weighted contributions (estimates of pass@k vs pass@1 inner products) demonstrate how pass@k reweighting *hurts pass@1*. Purple arrows highlight the critical downward shift from the unweighted mean (blue dotted, same as plot A) to the weighted mean (red dashed). **(a) Deepseek-Llama:** The downward shift from $+2.80 \times 10^{-3}$ to -1.12×10^{-3} ($\Delta = -3.92 \times 10^{-3}$) flips the gradient from positive to negative, resulting in inner product -0.613 . **(b) DeepSeek-Qwen:** The dramatic downward shift from $+2.97 \times 10^{-2}$ to -2.74×10^{-1} ($\Delta = -3.04 \times 10^{-1}$) demonstrates even stronger gradient conflict. Despite only 29 hard prompts vs 627 easy (21.6:1 ratio), the extreme weight disparity causes hard negatives to completely dominate, resulting in inner product -181 .

low-weight prompts cluster in the positive-agreement region. This means pass@k’s design, which correctly prioritizes hard prompts for its own objective, systematically amplifies negatively interfering prompts that hurt pass@1.

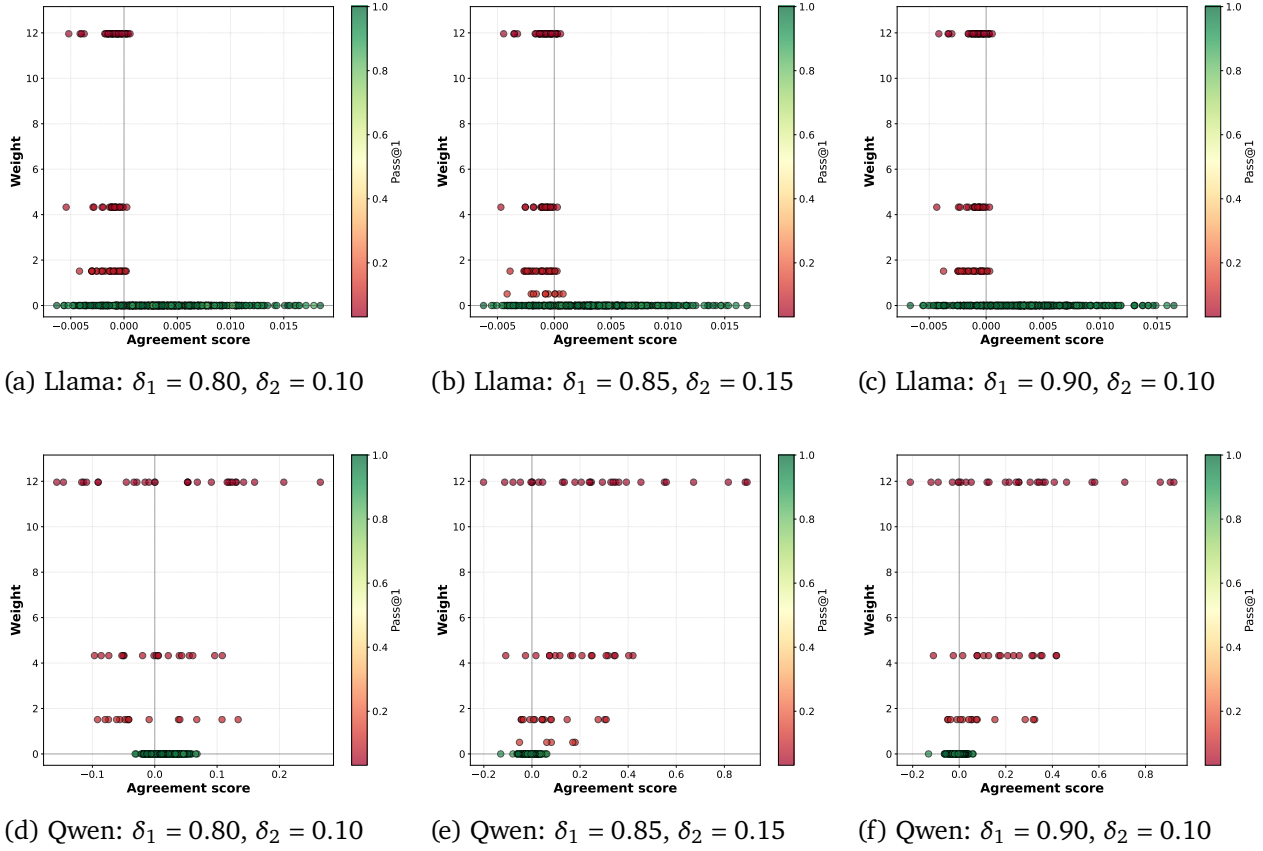


Figure 7 | **Pass@k amplification pattern across models and thresholds.** Each point represents one prompt, with the corresponding agreement score (x-axis), pass@k weight (y-axis), and pass@1 probability shown by color (red = low, green = high). **Consistent pattern:** Prompts with negative alignment (left), low pass@1 (red), and high weights (4-12) cluster upper-left, while prompts with positive alignment (right), high pass@1 (green), and zero weights ($\sim 10^{-28}$) appear lower-right. **Top row (a-c):** DeepSeek-R1-Distill-Llama-8B across three δ_2 values (0.05, 0.10, 0.15). **Bottom row (d-f):** DeepSeek-R1-Distill-Qwen-7B with same thresholds.

6. Related Work

Inference-time objective optimization has recently witnessed a surge of interest for optimizing language model performance for specific inference-time procedures such as win rate (Balashankar et al., 2025), Best-of-N (Amini et al., 2025; Aminian et al., 2025; Beirami et al., 2025; Chow et al., 2025; Sessa et al., 2025), majority voting (Du et al., 2025; Lightman et al., 2024; Uesato et al., 2022) or more recently their combination (Di et al., 2025). Davis and Recht (2025) showed that several existing algorithms for post-training large language models (such as rejection sampling fine-tuning (see e.g. Xiong et al. (2025)) and GRPO (Shao et al., 2024)) can be seen as instances of stochastic gradient ascent for maximizing a monotonically increasing function of the probability of giving a correct answer given a prompt, in the binary reward setting.

In this work, we focus on the special case of the pass@k metric which has been introduced as an

evaluation metric in [Chen et al. \(2021\)](#) for code generation tasks, similarly to a metric proposed earlier in [Kulal et al. \(2019\)](#). Given access to verifiable rewards, [Chen et al. \(2021\)](#) proposed an unbiased estimator of the pass@k metric. Inspired by inference-aware optimization gains, [Tang et al. \(2025\)](#) recently proposed to directly perform pass@k policy optimization with variance-reduced pass@k policy gradients using the control-variates method. Concurrently, [Walder and Karkhanis \(2025\)](#) introduced new lower variance unbiased estimators for pass@k and its gradient using more general U-statistics and demonstrated its performance for solving hard problems.

[Mahdavi et al. \(2025\)](#) derived expressions for the pass@k objective and pass@k policy gradients as presented in (2) and proposed a new pass@k gradient reweighting method with a tunable parameter γ different from k . [Yu \(2025\)](#) also derives per-prompt pass@k policy gradients and shows that per-prompt pass@k and pass@1 gradients are positively collinear vectors, questioning the soundness of considering the pass@k objective and advocating for different exploration mechanisms while keeping pass@k as an inference-time evaluation metric. We show in our work that the *expected* pass@k and pass@1 gradients over the prompt distribution may not necessarily be positively collinear.

[Chen et al. \(2025\)](#) investigated how pass@k model training balances the exploration and exploitation capabilities of large language models. [Jiang et al. \(2025\)](#) further considered a different risk-sensitive objective than pass@k based on a soft maximum (log-sum-exp) objective depending on a temperature parameter, providing a knob to trade-off between pass@k and pass@1 performance. [Peng et al. \(2025\)](#) proposed Simple Pass@K Optimization (SimKO) which redistributes gradient updates across the top-K token-level probability candidates to promote exploration and improve the balance between exploitation and exploration.

[Thrampoulidis et al. \(2025\)](#) connects policy gradient algorithms for pass@k optimization ([Mahdavi et al., 2025](#); [Tang et al., 2025](#); [Walder and Karkhanis, 2025](#)) to advantage shaped GRPO methods ([Chen et al., 2025](#); [Deng et al., 2025](#); [Mroueh, 2025](#); [Shao et al., 2024](#)).

To the best of our knowledge, among all prior work on pass@k optimization, our present work is the first to theoretically investigate the trade-off between pass@k and pass@1 under pass@k policy optimization.

7. Conclusion and Future Work

In this work, we investigated why pass@k policy optimization can degrade pass@1 showing that pass@k and pass@1 gradients can be conflicting when pass@k weights amplify negative prompt interference. Our findings open several avenues for future work. An immediate direction is to design and evaluate methods to mitigate this conflict issue. More broadly, it would be interesting to investigate more general inference-time objectives beyond pass@k (such as other concave transforms of the probability of success) in view of solving harder reasoning tasks and enhancing exploration with more flexible and targeted prompt reweighting without sacrificing pass@1 performance. Our similarity metric can offer a good starting point for gradient surgery.

References

- A. Amini, T. Vieira, E. Ash, and R. Cotterell. Variational best-of-n alignment. In *International Conference on Learning Representations*, 2025. 14
- G. Aminian, I. Shenfeld, A. R. Asadi, A. Beirami, and Y. Mroueh. Best-of-n through the smoothing lens: Kl divergence and regret analysis. *arXiv preprint arXiv:2507.05913*, 2025. 14

- A. Balashankar, Z. Sun, J. Berant, J. Eisenstein, M. Collins, A. Hutter, J. Lee, C. Nagpal, F. Prost, A. Sinha, A. T. Suresh, and A. Beirami. Inalign: Inference-aware language model alignment. In *International Conference on Machine Learning*, 2025. 14
- A. Beirami, A. Agarwal, J. Berant, A. N. D’Amour, J. Eisenstein, C. Nagpal, and A. T. Suresh. Theoretical guarantees on the best-of-n alignment policy. In *International Conference on Machine Learning*, 2025. 14
- M. Chen, J. Tworek, H. Jun, Q. Yuan, H. P. de Oliveira Pinto, J. Kaplan, H. Edwards, Y. Burda, N. Joseph, G. Brockman, A. Ray, R. Puri, G. Krueger, M. Petrov, H. Khlaaf, G. Sastry, P. Mishkin, B. Chan, S. Gray, N. Ryder, M. Pavlov, A. Power, L. Kaiser, M. Bavarian, C. Winter, P. Tillet, F. P. Such, D. Cummings, M. Plappert, F. Chantzis, E. Barnes, A. Herbert-Voss, W. H. Guss, A. Nichol, A. Paino, N. Tezak, J. Tang, I. Babuschkin, S. Balaji, S. Jain, W. Saunders, C. Hesse, A. N. Carr, J. Leike, J. Achiam, V. Misra, E. Morikawa, A. Radford, M. Knight, M. Brundage, M. Murati, K. Mayer, P. Welinder, B. McGrew, D. Amodei, S. McCandlish, I. Sutskever, and W. Zaremba. Evaluating large language models trained on code. *arXiv preprint arXiv:2107.03374*, 2021. 1, 12, 15
- Z. Chen, X. Qin, Y. Wu, Y. Ling, Q. Ye, W. X. Zhao, and G. Shi. Pass@ k training for adaptively balancing exploration and exploitation of large reasoning models. *arXiv preprint arXiv:2508.10751*, 2025. 15
- Y. Chow, G. Tennenholtz, I. Gur, V. Zhuang, B. Dai, A. Kumar, R. Agarwal, S. Thiagarajan, C. Boutilier, and A. Faust. Inference-aware fine-tuning for best-of-n sampling in large language models. In *International Conference on Learning Representations*, 2025. 14
- D. Davis and B. Recht. What is the objective of reasoning with reinforcement learning? *arXiv preprint arXiv:2510.13651*, 2025. 14
- W. Deng, Y. Ren, M. Li, D. J. Sutherland, X. Li, and C. Thrampoulidis. On the effect of negative gradient in group relative deep reinforcement optimization. In *Annual Conference on Neural Information Processing Systems*, 2025. 15
- Q. Di, K. Ji, X. Li, H. Zhao, and Q. Gu. Best-of-majority: Minimax-optimal strategy for pass@k inference scaling. *arXiv preprint arXiv:2510.03199*, 2025. 14
- W. Du, Y. Yang, and S. Welleck. Optimizing temperature for language models with multi-sample inference. *arXiv preprint arXiv:2502.05234*, 2025. 14
- J. Gehring, K. Zheng, J. Copet, V. Mella, T. Cohen, and G. Synnaeve. RLEF: Grounding code LLMs in execution feedback with reinforcement learning. In *International Conference on Machine Learning*, 2025. 1
- D. Hendrycks, C. Burns, S. Kadavath, A. Arora, S. Basart, E. Tang, D. Song, and J. Steinhardt. Measuring mathematical problem solving with the math dataset. *Advances in Neural Information Processing Systems*, 2021. 11
- Y. Jiang, J. Huang, Y. Yuan, X. Mao, Y. Yue, Q. Zhao, and L. Yan. Risk-sensitive rl for alleviating exploration dilemmas in large language models. *arXiv preprint arXiv:2509.24261*, 2025. 15
- S. Kulal, P. Pasupat, K. Chandra, M. Lee, O. Padon, A. Aiken, and P. S. Liang. Spoc: Search-based pseudocode to code. *Advances in Neural Information Processing Systems*, 32, 2019. 15
- Y. Li, D. Choi, J. Chung, N. Kushman, J. Schrittwieser, R. Leblond, T. Eccles, J. Keeling, F. Gimeno, A. Dal Lago, et al. Competition-level code generation with alphacode. *Science*, 378(6624):1092–1097, 2022. 1

- H. Lightman, V. Kosaraju, Y. Burda, H. Edwards, B. Baker, T. Lee, J. Leike, J. Schulman, I. Sutskever, and K. Cobbe. Let’s verify step by step. In *International Conference on Learning Representations*, 2024. 14
- S. Mahdavi, M. Li, K. Liu, R. Liao, and C. Thrampoulidis. Beyond accuracy: A policy gradient reweighting approach for pass@k maximization in LLMs. In *2nd AI for Math Workshop @ ICML 2025*, 2025. 4, 15
- Y. Mroueh. Reinforcement learning with verifiable rewards: Grpo’s effective loss, dynamics, and success amplification. *arXiv preprint arXiv:2503.06639*, 2025. 15
- M. Papini, M. Pirotta, and M. Restelli. Smoothing policies and safe policy gradients. *Machine Learning*, 111(11):4081–4137, 2022. 9
- R. Peng, Y. Ren, Z. Yu, W. Liu, and Y. Wen. Simko: Simple pass@k policy optimization. *arXiv preprint arXiv:2510.14807*, 2025. 15
- P. G. Sessa, R. Dadashi-Tazehozhi, L. Hussenot, J. Ferret, N. Vieillard, A. Rame, B. Shahriari, S. Perrin, A. L. Friesen, G. Cideron, S. Girgin, P. Stanczyk, A. Michi, D. Sinopalnikov, S. R. Garea, A. Héliou, A. Severyn, M. Hoffman, N. Momchev, and O. Bachem. BOND: Aligning LLMs with best-of-n distillation. In *International Conference on Learning Representations*, 2025. 14
- Z. Shao, P. Wang, Q. Zhu, R. Xu, J. Song, X. Bi, H. Zhang, M. Zhang, Y. Li, Y. Wu, et al. Deepseek-math: Pushing the limits of mathematical reasoning in open language models. *arXiv preprint arXiv:2402.03300*, 2024. 14, 15
- Y. Tang, K. Zheng, G. Synnaeve, and R. Munos. Optimizing language models for inference time objectives using reinforcement learning. In *International Conference on Machine Learning*, 2025. 1, 4, 15
- C. Thrampoulidis, S. Mahdavi, and W. Deng. Advantage shaping as surrogate reward maximization: Unifying pass@k policy gradients. *arXiv preprint arXiv:2510.23049*, 2025. 15
- J. Uesato, N. Kushman, R. Kumar, F. Song, N. Siegel, L. Wang, A. Creswell, G. Irving, and I. Higgins. Solving math word problems with process-and outcome-based feedback. *arXiv preprint arXiv:2211.14275*, 2022. 14
- C. Walder and D. T. Karkhanis. Pass@k policy optimization: Solving harder reinforcement learning problems. In *Annual Conference on Neural Information Processing Systems*, 2025. 1, 4, 12, 15
- W. Xiong, J. Yao, Y. Xu, B. Pang, L. Wang, D. Sahoo, J. Li, N. Jiang, T. Zhang, C. Xiong, and H. Dong. A minimalist approach to llm reasoning: from rejection sampling to reinforce. *arXiv preprint arXiv:2504.11343*, 2025. 14
- Y. Yu. Pass@k metric for rlvr: A diagnostic tool of exploration, but not an objective. *arXiv preprint arXiv:2511.16231*, 2025. 4, 15
- R. Yuan, R. M. Gower, and A. Lazaric. A general sample complexity analysis of vanilla policy gradient. In *International Conference on Artificial Intelligence and Statistics*, pages 3332–3380. PMLR, 2022. 9

Table of Contents

1	Introduction	1
2	Preliminaries	3
3	Prompt Interference	4
3.1	Prompt similarity measure and interference	4
3.2	Toy example	5
3.3	Tradeoff: pass@ k ascent can decrease pass@1	6
4	Pass@k and Pass@1 Gradients Conflict	7
4.1	Gradient conflict: Reweighting meets interference	7
4.2	Sufficient conditions and threshold in k	8
4.3	Pass@1 degradation under pass@ k updates	11
5	Experiments	11
6	Related Work	14
7	Conclusion and Future Work	15
A	Discussion of the covariance condition in Proposition 4.1	19
B	A kernel view of gradient conflict beyond $k = 1$	19
C	Proofs	19
C.1	Proof of Proposition 4.1: Gradients conflict characterization	19
C.2	Proof of Corollary 4.4: Dominating negatively interfering prompts	20
C.3	Proof of Proposition 4.5: Influence of k	21
C.4	Lemma C.1: Smoothness of pass@ k	21
C.5	Proof of Proposition 4.6: Pass@1 degradation under pass@ k updates	22
D	Additional Experiments	24
D.1	More details regarding experimental setting	24
D.2	Threshold robustness analysis	24

A. Discussion of the covariance condition in Proposition 4.1

Introducing the correlation $\rho_{w,a}(\theta) := \frac{\text{cov}(w_{k,\theta}(x), a_\theta(x))}{\sigma_w(\theta) \cdot \sigma_a(\theta)}$ where $\sigma_w(\theta)$, $\sigma_a(\theta)$ are respectively the standard deviations of $w_{k,\theta}(x)$ and $a_\theta(x)$, we can then rewrite condition (10) equivalently as:

$$\rho_{w,a}(\theta) < -\frac{\mathbb{E}[w_{k,\theta}(x)] \cdot \|\nabla J_1(\theta)\|^2}{\sigma_w(\theta) \cdot \sigma_a(\theta)}. \quad (19)$$

This condition emphasizes that conflict requires strong negative correlation between hardness weights and agreement scores as well as sufficient variance. If the weights barely vary ($\sigma_w(\theta) \simeq 0$), pass@k cannot strongly shift focus across prompts and conflict is harder. If agreement scores barely vary ($\sigma_a(\theta) \simeq 0$) there is no meaningful conflict structure to exploit that can lead to misaligned gradients.

B. A kernel view of gradient conflict beyond $k = 1$

In this section, we further investigate the gradient conflict phenomenon between pass@k and pass@m for any $k, m \geq 1$. Using the kernel κ_θ defined in (5), we now relate pass@k and pass@m gradients for any $k, m \geq 1$ using (2) to obtain:

$$\langle \nabla J_k(\theta), \nabla J_m(\theta) \rangle = \mathbb{E}_{x, x' \sim \mathcal{D}} [w_{k,\theta}(x) w_{m,\theta}(x') \kappa_\theta(x, x')]. \quad (20)$$

This identity separates two factors: (1) where each objective focuses via the weights $w_{k,\theta}(x)$, $w_{m,\theta}(x')$ with prompt reweighting toward ‘hard’ prompts as k grows; and (2) whether those regions interfere via the sign structure of $\kappa_\theta(x, x')$ which is independent of the parameter k . Conflict between pass@k and pass@m gradients happens when the objectives emphasize prompt regions whose cross-similarity (encoded by the kernel) is negative.

The following result which is an immediate consequence of (20) shows that conflict requires interference.

Proposition B.1 (No interference regime: No negative transfer \implies no conflict). *For any policy parameter $\theta \in \mathbb{R}^d$, if $\kappa_\theta(x, x') \geq 0$ for $\mathcal{D} \times \mathcal{D}$ a.e. (x, x') then, $\langle \nabla J_k(\theta), \nabla J_m(\theta) \rangle \geq 0$ for all $k, m \geq 1$.*

If pairwise prompt similarities are nonnegative on the support of the prompt distribution \mathcal{D} then all pass@k objectives are mutually aligned. Therefore, conflict can only occur when pairwise similarities are not always nonnegative and depends on how the weights $w_{k,\theta}$, $w_{m,\theta}$ shift mass. In other words, pass@k objectives cannot conflict unless there is negative transfer between some prompts.

C. Proofs

C.1. Proof of Proposition 4.1: Gradients conflict characterization

Proof. First recall from (2) that for any $k \geq 1$ and any $\theta \in \mathbb{R}^d$,

$$\nabla J_k(\theta) = \mathbb{E}_{x \sim \mathcal{D}} [w_k(p_\theta(x)) \nabla p_\theta(x)] = \mathbb{E}_{x \sim \mathcal{D}} [w_k(p_\theta(x)) \nabla J_1(x; \theta)]. \quad (21)$$

Then it immediately follows that:

$$\begin{aligned} \langle \nabla J_k(\theta), \nabla J_1(\theta) \rangle &= \langle \mathbb{E}_{x \sim \mathcal{D}} [w_k(p_\theta(x)) \nabla J_1(x; \theta)], \nabla J_1(\theta) \rangle \\ &= \mathbb{E}_{x \sim \mathcal{D}} [\langle w_k(p_\theta(x)) \nabla J_1(x; \theta), \nabla J_1(\theta) \rangle] \\ &= \mathbb{E}_{x \sim \mathcal{D}} [w_k(p_\theta(x)) a_\theta(x)], \end{aligned} \quad (22)$$

where we recall that $a_\theta(x) := \langle \nabla J_1(x; \theta), \nabla J_1(\theta) \rangle$. By definition of the covariance between two real-valued random variables:

$$\text{cov}(w_{k,\theta}(x), a_\theta(x)) = \mathbb{E}_{x \sim \mathcal{D}} [w_{k,\theta}(x) \cdot a_\theta(x)] - \mathbb{E}_{x \sim \mathcal{D}} [w_{k,\theta}(x)] \cdot \mathbb{E}_{x \sim \mathcal{D}} [a_\theta(x)] \quad (23)$$

$$= \langle \nabla J_k(\theta), \nabla J_1(\theta) \rangle - \mathbb{E}_{x \sim \mathcal{D}} [w_{k,\theta}(x)] \cdot \|\nabla J_1(\theta)\|^2, \quad (24)$$

where the second equality follows from using (22) and noticing that $\mathbb{E}_{x \sim \mathcal{D}} [a_\theta(x)] = \|\nabla J_1(\theta)\|^2$ by definition of $a_\theta(x)$. Rearranging the above identity then gives:

$$\langle \nabla J_k(\theta), \nabla J_1(\theta) \rangle = \mathbb{E}_{x \sim \mathcal{D}} [w_{k,\theta}(x)] \cdot \|\nabla J_1(\theta)\|^2 + \text{cov}(w_{k,\theta}(x), a_\theta(x)). \quad (25)$$

As a consequence of (22) and (25), we have that $\langle \nabla J_k(\theta), \nabla J_1(\theta) \rangle < 0$ if and only if: $\mathbb{E}_{x \sim \mathcal{D}} [w_{k,\theta}(x) a_\theta(x)] < 0$ which is also equivalent to the condition:

$$\text{cov}(w_{k,\theta}(x), a_\theta(x)) < -\mathbb{E}[w_{k,\theta}(x)] \cdot \|\nabla J_1(\theta)\|^2. \quad (26)$$

□

C.2. Proof of Corollary 4.4: Dominating negatively interfering prompts

Proof. First, Proposition 4.1 yields:

$$\langle \nabla J_k(\theta), \nabla J_1(\theta) \rangle = \mathbb{E}[\omega_{k,\theta}(x) a_\theta(x)]. \quad (27)$$

We decompose this inner product into 2 regions: the m -strongly negatively interfering region $\mathcal{X}_-(\theta, m)$ and its complement,

$$\langle \nabla J_k(\theta), \nabla J_1(\theta) \rangle = \mathbb{E}[\omega_{k,\theta}(x) a_\theta(x)] = \mathbb{E}[\omega_{k,\theta}(x) a_\theta(x) \mathbb{1}_{\{x \in \mathcal{X}_-(\theta, m)\}}] + \mathbb{E}[\omega_{k,\theta}(x) a_\theta(x) \mathbb{1}_{\{x \notin \mathcal{X}_-(\theta, m)\}}]. \quad (28)$$

We now upperbound each one of the above terms. For the first term, by definition of the set of prompts $\mathcal{X}_-(\theta, m)$, we have $a_\theta(x) \leq -m$ for any $x \in \mathcal{X}_-(\theta, m)$. As for the second term, we show that for any $x \notin \mathcal{X}_-(\theta, m)$, $|a_\theta(x)| \leq G^2$ using Assumption 4.3 as follows.

Bounding $a_\theta(x)$. Using the definition of the agreement score $a_\theta(x)$ (see (8)) together with Cauchy-Schwarz inequality, we have

$$a_\theta(x) = \langle \nabla J_1(x; \theta), \nabla J_1(\theta) \rangle \leq \|\nabla J_1(x; \theta)\| \cdot \|\mathbb{E}[\nabla J_1(x; \theta)]\| \leq \|\nabla J_1(x; \theta)\| \cdot \mathbb{E}[\|\nabla J_1(x; \theta)\|]. \quad (29)$$

Then recalling the policy gradient expression of $\nabla J_1(x; \theta)$ in (4) and using Jensen's inequality, we have:

$$\|\nabla J_1(x; \theta)\|^2 = \|\mathbb{E}_{y \sim \pi_\theta(\cdot|x)} [r(x, y) s_\theta(x, y)]\|^2 \leq \mathbb{E}_{y \sim \pi_\theta(\cdot|x)} [\|s_\theta(x, y)\|^2] \leq G^2, \quad (30)$$

where the last inequality follows from using Assumption 4.3. Using this inequality in (29) yields the desired inequality:

$$\forall x \in \mathcal{X}, \quad |a_\theta(x)| \leq G^2. \quad (31)$$

Back to (28) and using the inequalities established above, we conclude the proof:

$$\langle \nabla J_k(\theta), \nabla J_1(\theta) \rangle \leq -\delta(\theta), \quad (32)$$

where $\delta(\theta) := mW_-(k, \theta) - G^2W_+(k, \theta)$ and the aggregated weights $W_-(k, \theta), W_+(k, \theta)$ are defined in (14). If in addition $\delta(\theta) < 0$, then $\langle \nabla J_k(\theta), \nabla J_1(\theta) \rangle \leq -\delta(\theta) < 0$. □

C.3. Proof of Proposition 4.5: Influence of k

Proof. Recall from Proposition 4.1 that:

$$\langle \nabla J_k(\theta), \nabla J_1(\theta) \rangle = \mathbb{E}[\omega_{k,\theta}(x) a_\theta(x)] . \quad (33)$$

Using again the same decomposition as in (28), we have:

$$\langle \nabla J_k(\theta), \nabla J_1(\theta) \rangle = \mathbb{E}[\omega_{k,\theta}(x) a_\theta(x)] = \mathbb{E}[\omega_{k,\theta}(x) a_\theta(x) \mathbb{1}_{\{x \in \mathcal{X}_-(\theta, m)\}}] + \mathbb{E}[\omega_{k,\theta}(x) a_\theta(x) \mathbb{1}_{\{x \notin \mathcal{X}_-(\theta, m)\}}] . \quad (34)$$

Depending on the prompt region, we have two distinct ways to bound the pass@k weights:

- (i) For $x \in \mathcal{X}(m, \theta)$, we have by assumption, $p_\theta(x) \leq \varepsilon$, hence $\omega_{k,\theta}(x) \geq k(1 - \varepsilon)^{k-1}$.
- (ii) For $x \notin \mathcal{X}(m, \theta)$ we have by assumption, $p_\theta(x) \geq \delta$, hence $\omega_{k,\theta}(x) \leq k(1 - \delta)^{k-1}$.

Observing in addition to both items above that $a_\theta(x) \leq -m$ for any $x \in \mathcal{X}_-(\theta, m)$ and $a_\theta(x) \leq G^2$ for any $x \in \mathcal{X}$ (as shown in (31) under Assumption 4.3) and hence for any $x \notin \mathcal{X}_-(\theta, m)$ in particular, we obtain from (34) the following inequality:

$$\langle \nabla J_k(\theta), \nabla J_1(\theta) \rangle \leq -k(1 - \varepsilon)^{k-1} m q + k(1 - \delta)^{k-1} G^2 (1 - q) , \quad (35)$$

where we also use the assumption $q_\theta > q$. Thus it suffices to have

$$k(1 - \delta)^{k-1} G^2 (1 - q) < k(1 - \varepsilon)^{k-1} m q ,$$

to ensure that $\langle \nabla J_k(\theta), \nabla J_1(\theta) \rangle < 0$. The above condition is equivalent to:

$$\frac{G^2(1 - q)}{m q} < \left(\frac{1 - \varepsilon}{1 - \delta} \right)^{k-1} .$$

Taking log in the above inequality, recalling that $1 - \varepsilon > 1 - \delta$ and reordering the inequality yields:

$$k > k^* := 1 + \frac{\log\left(\frac{(1 - q) G^2}{q m}\right)}{\log\left(\frac{1 - \varepsilon}{1 - \delta}\right)} , \quad (36)$$

which concludes the proof. \square

C.4. Lemma C.1: Smoothness of pass@k

Lemma C.1 (Smoothness of pass@k). *Under Assumption 4.3, for all $k \geq 1$, the pass@k objective J_k is L_k -smooth with $L_k := k^2 G^2 + kF$, i.e. for all $\theta, \theta' \in \mathbb{R}^d$,*

$$|J_k(\theta') - J_k(\theta) - \langle \nabla J_k(\theta), \theta' - \theta \rangle| \leq \frac{L_k}{2} \|\theta' - \theta\|_2^2 .$$

Proof. To show smoothness of the pass@k objective J_k , we bound its Hessian $\nabla^2 J_k(\theta)$ uniformly in the policy parameter θ using Assumption 4.3.

Since $\nabla J_k(\theta) = \mathbb{E}_{x \sim \mathcal{D}}[w_k(p_\theta(x)) \nabla p_\theta(x)]$ as shown in (2), the chain rule gives the Hessian of J_k for every $\theta \in \mathbb{R}^d$,

$$\nabla^2 J_k(\theta) = \mathbb{E}_{x \sim \mathcal{D}} \left[\omega'_k(p_\theta(x)) \nabla p_\theta(x) \nabla p_\theta(x)^\top + \omega_k(p_\theta(x)) \nabla^2 p_\theta(x) \right] . \quad (37)$$

Taking the operator norm and using the triangular inequality yields:

$$\|\nabla^2 J_k(\theta)\| \leq \mathbb{E}_{x \sim \mathcal{D}} \left[|\omega'_k(p_\theta(x))| \cdot \|\nabla p_\theta(x)\|^2 + |\omega_k(p_\theta(x))| \cdot \|\nabla^2 p_\theta(x)\| \right] . \quad (38)$$

In the rest of the proof, we bound each term separately.

Step 1: Bounding $\|\nabla p_\theta(x)\|^2$. Recall from (4) that the pass@1 policy gradient is given by:

$$\nabla p_\theta(x) = \mathbb{E}_{y \sim \pi_\theta(\cdot|x)} \left[r(x, y) \nabla \log \pi_\theta(y|x) \right]. \quad (39)$$

By Jensen's inequality and since $r(x, y) \in \{0, 1\}$, we have

$$\|\nabla p_\theta(x)\|^2 \leq \mathbb{E}_{y \sim \pi_\theta(\cdot|x)} \left[r(x, y)^2 \|\nabla \log \pi_\theta(y|x)\|^2 \right] \leq \mathbb{E}_{y \sim \pi_\theta(\cdot|x)} \left[\|\nabla \log \pi_\theta(y|x)\|^2 \right] \leq G^2, \quad (40)$$

where the last bound follows from Assumption 4.3.

Step 2: Bounding $\|\nabla^2 p_\theta(x)\|$. Differentiating the pass@1 policy gradient, we obtain:

$$\nabla^2 p_\theta(x) = \mathbb{E}_{y \sim \pi_\theta(\cdot|x)} \left[r(x, y) \nabla \log \pi_\theta(y|x) \nabla \log \pi_\theta(y|x)^\top + r(x, y) \nabla^2 \log \pi_\theta(y|x) \right].$$

Taking the operator norm and using the triangle inequality, we obtain:

$$\begin{aligned} \|\nabla^2 p_\theta(x)\| &\leq \mathbb{E}_{y \sim \pi_\theta(\cdot|x)} \left[|r(x, y)| \cdot \|\nabla \log \pi_\theta(y|x)\|^2 \right] + \mathbb{E}_{y \sim \pi_\theta(\cdot|x)} \left[|r(x, y)| \cdot \|\nabla^2 \log \pi_\theta(y|x)\| \right] \\ &\leq \mathbb{E}_{y \sim \pi_\theta(\cdot|x)} \left[\|\nabla \log \pi_\theta(y|x)\|^2 \right] + \mathbb{E}_{y \sim \pi_\theta(\cdot|x)} \left[\|\nabla^2 \log \pi_\theta(y|x)\| \right] \leq G^2 + F, \end{aligned} \quad (41)$$

where the last inequality again follows from using Assumption 4.3.

Step 3: Bounding weights ω'_k and ω_k . By definition of the weights $w_k(p) = f'_k(p) = k(1-p)^{k-1}$ for any $p \in [0, 1]$. Therefore it follows that $\omega'_k(p) = -k(k-1)(1-p)^{k-2}$ for $k \geq 2$. Hence, for any $p \in [0, 1]$ and any $k \geq 2$,

$$|\omega_k(p)| \leq k, \quad |\omega'_k(p)| \leq k(k-1). \quad (42)$$

Conclusion. Plugging (40)–(41) and the bounds on ω_k, ω'_k (42) into (38) yields

$$\|\nabla^2 J_k(\theta)\| \leq k(k-1)G^2 + k(G^2 + F) \leq k^2G^2 + kF.$$

Finally, boundedness of the Hessian norm implies that J_k is L_k -smooth with $L_k = k^2G^2 + kF$, i.e., for any $\theta, \theta' \in \mathbb{R}^d$,

$$\left| J_k(\theta') - J_k(\theta) - \langle \nabla J_k(\theta), \theta' - \theta \rangle \right| \leq \frac{L_k}{2} \|\theta' - \theta\|^2.$$

□

C.5. Proof of Proposition 4.6: Pass@1 degradation under pass@k updates

Proof. We prove the decrease of pass@1 and increase of pass@k under pass@k policy gradient ascent separately. Recall the policy update rule with step size $\eta > 0$:

$$\theta^+ = \theta + \eta \nabla J_k(\theta). \quad (43)$$

(i) Pass@1 descent. By L_1 -smoothness of J_1 (Lemma C.1) and using the policy update rule (43), we have:

$$\begin{aligned} J_1(\theta^+) &\leq J_1(\theta) + \langle \nabla J_1(\theta), \theta^+ - \theta \rangle + \frac{L_1}{2} \|\theta^+ - \theta\|^2 \\ &= J_1(\theta) + \eta \langle \nabla J_1(\theta), \nabla J_k(\theta) \rangle + \frac{L_1 \eta^2}{2} \|\nabla J_k(\theta)\|^2. \end{aligned} \quad (44)$$

We now bound each one of the last two terms in the above inequality.

Bounding $\|\nabla J_k(\theta)\|^2$. Recall the pass@k policy gradient expression $\nabla J_k(\theta) = \mathbb{E}_x[\omega_\theta(x) \nabla J_1(x; \theta)]$, we have by Jensen and Cauchy-Schwarz inequalities:

$$\|\nabla J_k(\theta)\|^2 = \|\mathbb{E}_x[\omega_\theta(x) \nabla J_1(x; \theta)]\|^2 \leq \mathbb{E}_x[|\omega_\theta(x)|^2 \|\nabla J_1(x; \theta)\|^2] \leq k^2 G^2, \quad (45)$$

where the last inequality follows from using the pass@1 policy gradient bound in (30) together with immediate weight bound $|\omega_\theta(x)| \leq k$ and the fact that the reward is binary (this can be generalized to a continuous uniformly bounded reward function).

Bounding $\langle \nabla J_1(\theta), \nabla J_k(\theta) \rangle$. By Corollary 4.4, we have

$$\langle \nabla J_1(\theta), \nabla J_k(\theta) \rangle \leq -\delta(\theta). \quad (46)$$

Combining the bounds (45) and (46), we immediately obtain from (44):

$$J_1(\theta^+) \leq J_1(\theta) - \eta\delta(\theta) + C_2\eta^2, \quad (47)$$

where $C_2 := \frac{L_1 k^2 G^2}{2}$ and $L_1 = G^2 + F$ as shown in Lemma C.1, G, F being smoothness constants defined in Assumption 4.3.

Hence, if $\delta(\theta) > 0$ and $0 < \eta \leq \eta_+ := \frac{\delta(\theta)}{C_2}$, then $-\eta\delta(\theta) + C_2\eta^2 < 0$ and it follows that

$$J_1(\theta^+) \leq J_1(\theta) - \eta\delta(\theta) + C_2\eta^2 < J_1(\theta), \quad (48)$$

which is the first desired inequality.

(ii) Pass@k ascent. As for pass@k under pass@k policy gradient ascent, the proof is a standard application of smoothness in optimization. We provide a brief proof in our setting for completeness.

Using L_k -smoothness of the pass@k objective shown in Lemma C.1 together with the policy update rule (43), we have:

$$\begin{aligned} J_k(\theta^+) &\geq J_k(\theta) + \langle \nabla J_k(\theta), \theta^+ - \theta \rangle - \frac{L_k}{2} \|\theta^+ - \theta\|^2 \\ &= J_k(\theta) + \eta \|\nabla J_k(\theta)\|^2 - \frac{L_k \eta^2}{2} \|\nabla J_k(\theta)\|^2 \\ &= J_k(\theta) + \eta \left(1 - \frac{L_k \eta}{2}\right) \|\nabla J_k(\theta)\|^2. \end{aligned} \quad (49)$$

We pick then $\eta \leq \frac{1}{L_k}$ to obtain the second desired inequality:

$$J_k(\theta^+) \geq J_k(\theta) + \frac{\eta}{2} \|\nabla J_k(\theta)\|^2 \geq J_k(\theta). \quad (50)$$

Overall, a sufficient step-size condition to guarantee simultaneous increase of pass@k and decrease of pass@1 (i.e., in particular $J_1(\theta^+) < J_1(\theta)$ and $J_k(\theta^+) > J_k(\theta)$ when $\nabla J_k(\theta) \neq 0$) is:

$$0 < \eta \leq \min\left(\frac{\delta(\theta)}{C_2}, \frac{1}{L_k}\right), \quad (51)$$

and this concludes the proof. \square

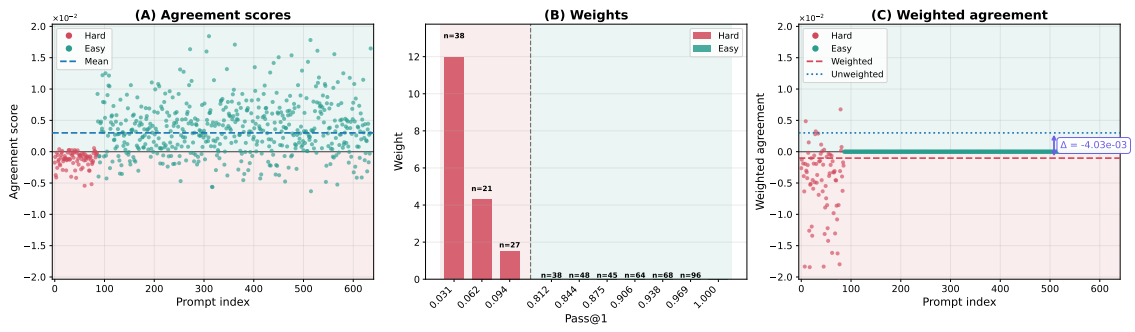
D. Additional Experiments

D.1. More details regarding experimental setting

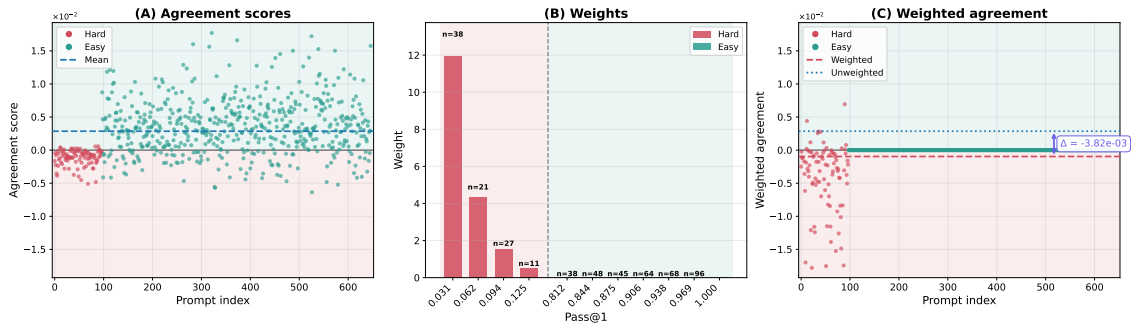
Sampling configuration. For each problem, we generate $k = 32$ independent responses using temperature sampling with temperature $T = 0.7$ and nucleus sampling with $p = 0.95$. Responses are evaluated using exact match against ground truth answers and binary rewards indicate correctness.

D.2. Threshold robustness analysis

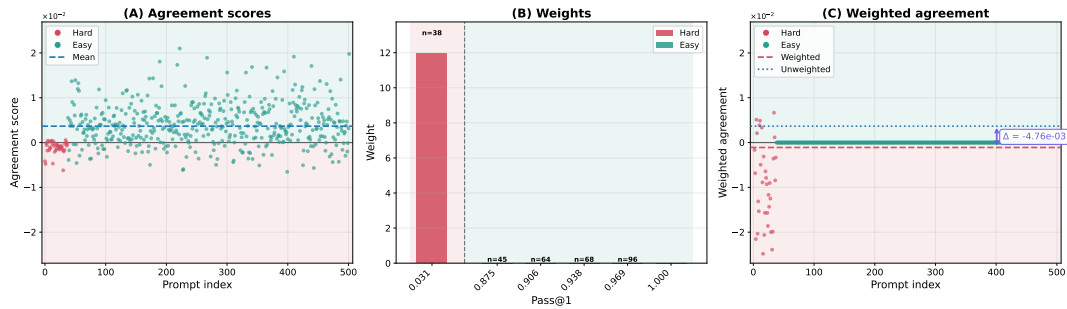
Figure 8 shows gradient misalignment across all 6 additional threshold configurations for DeepSeek-R1-Distill-Llama-8B (beyond the main text example of $\delta_1 = 0.85$, $\delta_2 = 0.10$). All combinations exhibit negative inner products (range: -0.49 to -0.65), demonstrating that the misalignment phenomenon is robust to threshold choices.



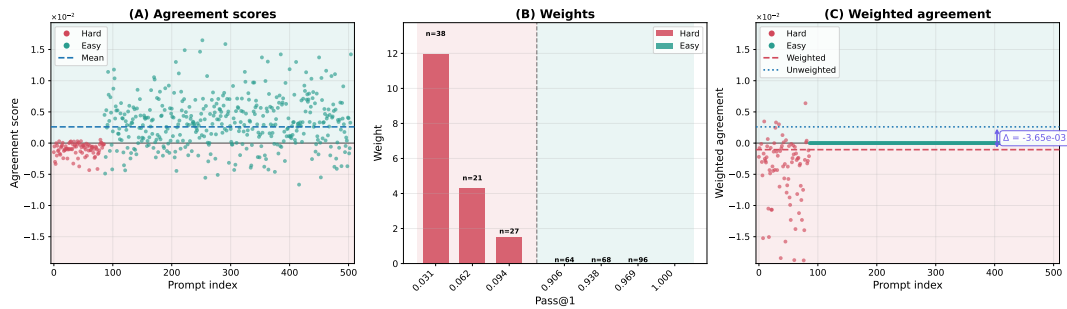
(a) $\delta_1 = 0.80, \delta_2 = 0.10$ (636 prompts: 86 hard, 550 easy, IP=-0.652)



(b) $\delta_1 = 0.80, \delta_2 = 0.15$ (647 prompts: 97 hard, 550 easy, IP=-0.621)



(c) $\delta_1 = 0.85, \delta_2 = 0.05$ (502 prompts: 38 hard, 464 easy, IP=-0.551)



(d) $\delta_1 = 0.90, \delta_2 = 0.10$ (505 prompts: 86 hard, 419 easy, IP=-0.527)

Figure 8 | Gradient conflict across all threshold configurations (DeepSeek-R1-Distill-Llama-8B). Each panel shows agreement scores, weights, and weighted contributions for a different (δ_1, δ_2) configuration. All exhibit negative inner products, confirming robust misalignment across thresholds. The consistent downward shift from unweighted to weighted means shows pass@k optimization systematically opposes pass@1 improvement.